# Green Synthesis of Silver Nanoparticles using *Lawsonia inermis* for Enhanced Degradation of Organic Pollutants in Wastewater Treatment

**Natrayan L[1,*], Jayakrishna M[2], Shanker K.[3], Muthu G[4], Kaliappan S.[5], Velmurugan G.[6]**

[1]Department of Mechanical Engineering, Saveetha School of Engineering, SIMATS, Chennai, Tamil Nadu, India - 602 105.

[2]Department of Mechanical Engineering, Sri Sivani Engineering College, Etcherla, Chilakapalem, Andhra Pradesh 532402

[3]Kamala Institute of Technology and Science, Singapur, Karimnagar, Telangana – 505468, India

[4]Department of Mechanical Engineering, Rajalakshmi Institute of Technology, Kuthampakkam, Chennai 600124, Tamil Nadu, India

[5]Department of Mechatronics Engineering, KCG College of Technology, Karapakkam, Chennai-600097, Tamil Nadu, India

[6]Institute of Agricultural Engineering, Saveetha School of Engineering, SIMATS, 602 105, Chennai, Tamil Nadu, India

[*]Corresponding author: email: natrayanphd@gmail.com.

## GRAPHICAL ABSTRACT

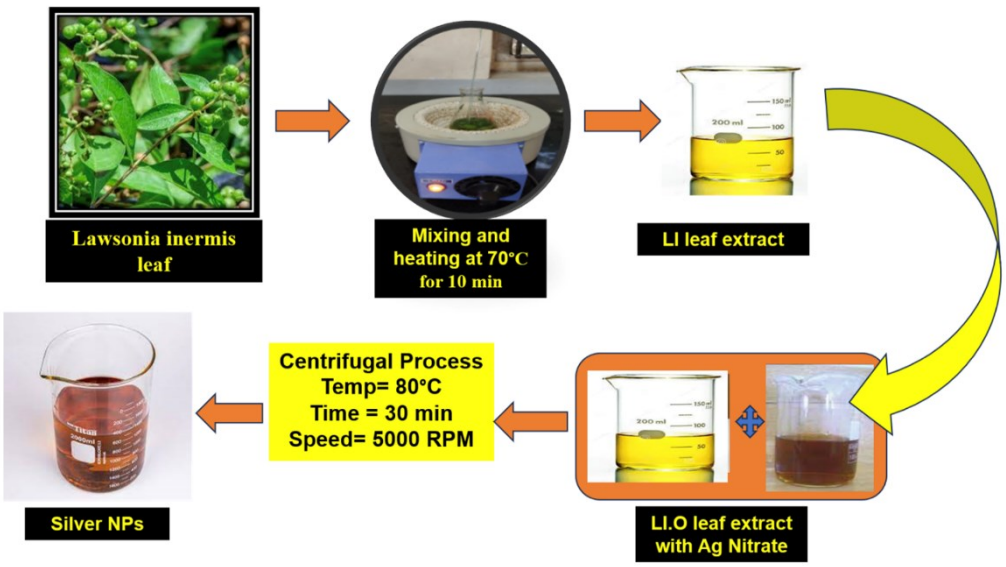


## Abstract

In response to the growing demand for eco-friendly and efficient catalysts in wastewater treatment, this study introduces a novel, biosynthesized silver nanoparticle (AgNP) using leaf extract from Lawsonia inermis, a widely available plant. We employed a unique concentration mixture of 0.015 mg/mL leaf extract and 2.0 mM silver nitrate to achieve optimal results under atmospheric conditions. Comprehensive characterization was conducted through X-ray

diffraction, transmission electron microscopy, scanning electron microscopy, and ultraviolet-visible absorption spectroscopy. Remarkably, these Lawsonia inermis-synthesized AgNPs (LI-AgNPs) demonstrated superior catalytic degradation of organic pollutants, such as 4-nitrophenol, methylene blue, eosin yellow, and methyl orange. Among them, 4-nitrophenol was reduced most efficiently, following pseudo-first order kinetics. The LI-AgNPs exhibited unprecedented catalytic potential, evidenced by a sharp decline in methyl orange absorption and the emergence of a new hydrazine compound signal at 280 nm. With a catalytic loading as low as 0.2 mg/mL, we achieved an astounding 82.5% dye removal. This innovative approach advances the field of environmental remediation and offers a sustainable and cost-effective solution for water purification applications.

**Keywords:** Green Synthesis, Water Pollutants, Catalytic Reduction, Wastewater treatment, Lawsonia inermis, Siver nitrate.

## 1. Introduction

The potential uses of ecologically friendly technologies for manufacturing silver nanoparticles (AgNPs) in wastewater treatment have garnered significant interest. A popular medicinal plant called Lawsonia inermis has shown great promise as a green synthesis material, offering an environmentally friendly substitute for traditional chemical processes. Lawsonia inermis leaves have a rich phytochemical composition, which has been emphasized in previous research. In particular, its active chemicals possess reducing and stabilizing capabilities, which makes it a perfect option for the environmentally friendly synthesis of AgNPs [1]. In addition to being in line with green chemistry principles, producing nanoparticles using plant extracts also eliminates the necessity for dangerous reducing chemicals. According to published research, AgNPs made using Lawsonia inermis may have special qualities that enable them to work as efficient catalysts for the breakdown of certain organic pollutants found in wastewater, such as methyl orange, 4-nitrophenol, methylene blue, and eosin yellow. An intriguing direction for environmental and nanotechnology research is to investigate the green synthesis of AgNPs from Lawsonia inermis, since the need for sustainable and effective wastewater treatment solutions continues to rise [2].

Due to their substantial variation, the abundance of severely undercoordinated interface places, and the demonstration of the quantum confinement phenomenon that significantly alters their response, noble metal nanocrystals are the foreseeable future of nanoparticles for heterogeneous catalytic processes [3]. Silver nanoparticles (AgNPs) are actively investigated as redox catalysts in addition to their multiple uses in biomolecular diagnosis, therapies, and

microelectronics since they have addressed the basic issue of size impact in catalysts [4, 5]. They also have a very high surface area, a regenerative microelectrode surface, and microelectrode potentials that are continually changing, making them desirable as catalysts. Due to the lower fermi attraction to silver particles in the nanoscale domain, such nanoscale groups can move radicals through the particle-solution interaction in a manner comparable to electrode processes [6]. Nanosilver colloidal contains an elevated surface plasma resonance (SPR) region in the visible spectrum that is particularly sensitive to exterior absorption; therefore, any absorption impact might be detected spectrophotometrically. This makes it different from other metallic nanomaterials [7]. In recognition of their high productivity, various chemical, biological, and physical reactions are commonly used to create silver nanoparticles. The problem of the cytotoxicity of silver nanoparticles on human beings and their surroundings has been elevated nonetheless due to the substantial use of aggressive substances and demanding laboratory conditions in these processes. Due to its straightforward, ecologically conscious, and cost-effective procedures founded on chemically safe solvents, risk-free substances, and renewable resources, sustainability in nanotechnology has attracted tremendous interest [8]. To produce nanosilver colloids, various naturally occurring sources, including extracts of plants and phytochemicals such as microorganisms, seaweed, and algal cells, have shown promise. Plant extracts are used in bio-inspired methods that are very easy to use and produce a wide range of nanomaterials in size and form. According to reports, additional metabolites of plants like phenol compounds, alkaloid substances, terpenoids, and polyphenols significantly contribute to the decrease of silver ions in the atmosphere and the subsequent creation of nanomaterials [9, 10]. The responsiveness of natural tiny silver colloids, which have become widespread in wastewater rehabilitation, ecology, biomedicine, medical care, farming, commercial gadgets, detectors, solar power, and clothing, is significantly influenced by phytonutrients.

Significant global social and economic development has led to a rapid exhaustion of freshwater supplies, which calls for the handling and regenerating of wastewater from industries and prudent utilization of already available supplies. The main industrial chemicals immediately impacting the natural world are synthesized organic substances widely used in industries. Numerous biological and chemical techniques can eliminate these contaminants, including absorption, ozonation photography, microwave-based deterioration, chemical catalytic processes, the Fenton response, and electrocatalysis [11]. The primary weakness of these treatments is their high cost and significant energy use throughout recovery. Furthermore, most current techniques transmit toxins from one stage to another, resulting in subsequent

contamination [12]. The application of nanomaterials in actual cleanup techniques for contaminants has increased recently. One of the more current fields of study in the water treatment industry is the enzymatic elimination of contaminants using biological nanomaterials. In a modern setting, such nanostructures provide enhanced, safe, and affordable cleaning techniques for remediating environments [13, 14]. Chemical contaminants known as nitrophenols are employed in producing pharmaceuticals, pesticides, and pyrotechnics. The American Ecological Protection Agency has designated 129 organic substances as dangerous to people and the planet, including four-nitrophenol (4NP). Due to its high water solubility, it is widely distributed in soil and wastewater from industries. Therefore, any meaningful contribution to the detoxification of 4NP is crucial for the ecosystem and industry. For the catalytic decomposition of 4-nitrophenol, iron nanoparticles immobilized in sphere polyelectrolyte brushing were used [15]. It was discovered that the kinetics of the 4-nitrophenol elimination by the nanoparticles of silver and gold stabilized on alginate-based calcium hydrogel pellets were out of order. According to Gangula et al., Breynia rhamnoides-mediated biological metallic nanomaterials effectively reduced 4NP. The amount of 4-nitrophenol (4-NP) was decreased via a Fenton-like process on nano-zero-valent metal. A significant family of organic compounds called dyes is widely used in contemporary industry [16]. A significant environmental issue is the large-scale dumping of unprocessed colored manmade dye-based contaminants from the paper, drugs, painting, textiles, plastics, aesthetically pleasing, and food sectors. By preventing sunlight penetration, lowering oxygenation ability, and generating a process known as colored contaminants, these contaminants disrupt the aquatic ecology. Additionally, because they are cancerous and mutation-causing, pesticides seriously harm humans. Most colors are durable and immune to oxidizing chemicals, light, or oxidative digestion's deterioration.

Methylene blue (MB) is a thiazine electrostatic pigment that, in its oxidized condition, displays a rich blue colour and is colorless in its reduced form. Due to its intricate artificial order, which prevents it from degrading and makes it immune to the effects of its surroundings, it is a durable pigment that is hard to remove. Both photocatalytic degradation and enzymatic staining of MB have been reported in research [17, 18]. Tetrabromofluorescein pigment, known as eosin yellow (EY), is water-based and has several uses in the paper and garment sectors. Researchers used natural metallic nanoparticles and their conjugates to eliminate this organic contaminant. Azo colorants which can cause cancer are used extensively in industry and are therefore a necessary component of decomposing waters [19]. Lawsonia inermis, sometimes

known as henna, is a Lythraceae small plant species. Usually, L. inermis is used in conventional medicines worldwide to cure a broad spectrum of illnesses, including edoema, asthma, arthritis, smallpox, spermatorrhoea, irregular menstrual periods, and haemorrhoids. Lawson, a primary colourant found in L. inermis, lends a light yellow to red hue depending on the dying circumstances and material type. L. inermis comprises various biological molecules, making it a valuable source for several medications. Lawsoniasides, gallic acids, flavonoids, quinoids, chemical swaps, chemical compounds, and coumarins are a group of compounds, and polyphenol amino acids are among the main components of L. inermis [20].

The current paper details our attempts to synthesize AgNPs utilising verifiably sustainable chemical concepts and L. inermis leaf extract as a stand-alone reduction and cap reagent. Because of its therapeutic use, this physiological elimination of silver might be advantageous for creating additional nanomaterials [21]. This work presents a simple, one-pot approach for producing biologically generated AgNPs that can reduce organic contaminants by catalyzing the degradation of the Lawsonia inermis leaf extract. The impact of many variables was assessed, including pH, silver concentration in salt water, and leaf extract percentage. Ultraviolet spectroscopy (UV), Transmission electron microscopy (TEM), FTIR, and X-ray diffraction (XRD) analyses were used to characterize the synthesized leaf extract-based metallic nanoparticles. For environmentally conscious oxidative enzymes for facilitating the elimination of organic contaminants in waste water, leaf extract-based silver nanoparticles have been utilised, and the resulting kinetics were examined.

## 2. Experimental Works

### 2.1 Materials

In the course of this investigation, various chemicals such as Methyl orange, silver nitrate, sodium borohydride, eosin yellow, sodium hydroxide, and 4-nitrophenol, along with all the requisite solutions, were procured from Rithu Chemicals Private Limited. The aqueous solutions were meticulously prepared using distilled water, and all compounds were employed without prior filtration. Notably, the glassware underwent thorough cleaning and rinsing with disinfected water before usage to prevent contamination. This meticulous approach ensures the reliability of the experimental results by maintaining the purity of the reagents and the cleanliness of the experimental setup.

### 2.2 Preparation of Leaf Extract and Nanoparticle

Fresh leaves of Lawsonia inermis (L. inermis) were harvested from the botanical park on Saveetha University's campus in Chennai, India. The green leaves were carefully collected and thoroughly cleaned using water from the faucet and Milli-Q solution to eliminate any impurities. Following the cleaning process, the leaves were meticulously dried in darkness to ensure the removal of humidity. The dried leaves were then finely ground into a powder using an electrical blender. The resulting powder (5 g) underwent sieving before being mixed with 100 ml of Milli-Q water and heated at 70 °C for 10 minutes. To isolate the extracted leaves (LI), Whatman's No. 1 filtration paper was employed. The resulting filtrate, containing the extracted components, was then preserved at 5 °C for further use in the production of silver nanoparticles (AgNPs). This detailed process outlines the careful collection, preparation, and extraction steps involved in utilizing Lawsonia inermis leaves to produce AgNPs, highlighting the precision and methodology employed in the study.

**2.3 Biosynthesis of Silver Nanoparticle**

In the biosynthetic studies conducted, 5.0 mL of silver nitrate solution and 10.0 mL of plant extract were prepared in a water solution. To expedite the process, a solution of sodium hydroxide (1 M, 100 L) was introduced as an accelerator, enhancing the reduced power of macromolecules and consequently accelerating the overall reaction. The mixture, maintained at ambient temperature, underwent slow stirring (50 rpm) until the liquid's color transitioned from yellow to brown, indicating the formation of minute silver particles. The stability of the silver progenitor solution was carefully maintained at 0.5 mM throughout the process. Varying doses within the 0.016 g/mL range were examined to investigate the influence of the plant extract on nanosilver production. Additionally, biosynthesis experiments were conducted using silver salts ranging from 1.0 to 2.5 mM, while the leaf extract was consistently held at 0.015 g/mL. Multiple pH values within the range of 6-7 were employed during the synthesis process to achieve a silver colloid with a precise size range. Following synthesis, the homogeneous nanoproduct was isolated through centrifugation at 5000 rpm for 30 minutes, followed by thorough rinsing with fresh water multiple times. Figure 1 provides a visual representation of the biosynthesis process of silver nanoparticles.

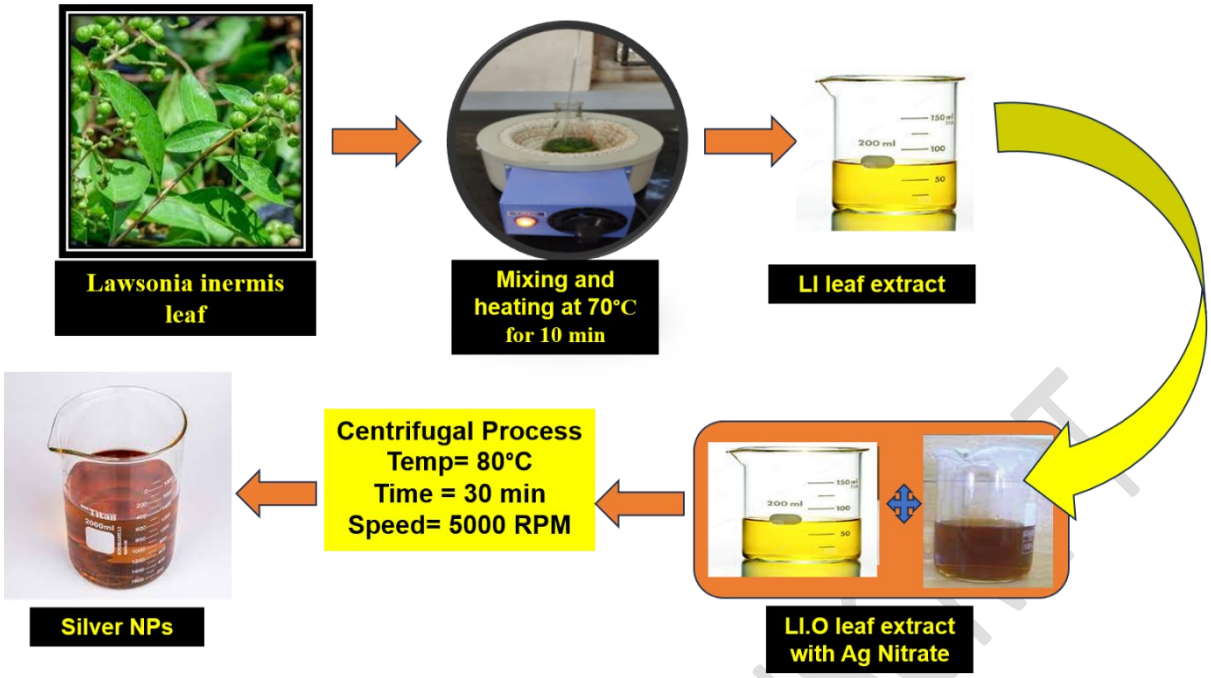


**Figure 1.** Biosynthesis of Silver NPs from lawsonia inermis leaf

### 2.4 Characterization

XRD with Cu K radiations has been utilized to identify the crystallographic character of nanosilver by scanning in the area of 2Θ from 10 degrees to 80 degrees to analyze the crystal structures of silver particles. Field emission scanning electron microscopic examination (SEM) was conducted utilizing all HRSEM Apreo 3. In contrast, the field-emission transmission electron microscopy (TEM) version JEOL JEM 2100 plus had been used to perform morphology examinations. At 10-minute intervals following the incorporation of the colloids, the concentration-related catalyzed properties of leaf extract-based AgNPs have been determined through UV-visible spectroscopy.

### 2.5 Catalytic activity of nano silver

Four distinct contaminants, including 4NP, EY, MO, and MB, have been used as research reagents to assess the reactive catalytic capability of synthesized nanomaterials. 0.2 mL of solution (1.0 mM) for each contaminant was incorporated into 0.2 mL of $NaBH_4$ solution (0.5 M). In every study, estimated doses of a leaf extract-based AgNP colloidal (1 mg/mL) were employed to obtain the appropriate levels. The identical methodology was followed for control studies; however, silver nanoparticles weren't used. The reacted mixture was continuously stirred for five minutes; afterward, its capacity increased to 6.0 mL. Information was acquired from 20 min up to 70 min, measuring time-dependent reductions in the catalyst by spectroscopy

for the experiment and control fluids as a function of variation in absorption across the entire exposure duration.

## 3. Result and discussion

### 3.1 Microstructural analysis of AgNPs

The dimension, form, and morphological features of LI-AgNPs were determined using transmission electron microscopy since the inherent qualities of nanomaterials vary with their structural makeup. The internal structure of the synthesized nanoparticles was virtually spherical, as shown in TEM pictures (Figure 2). The nanoparticles' median dimension was determined to be 30.12 nm.

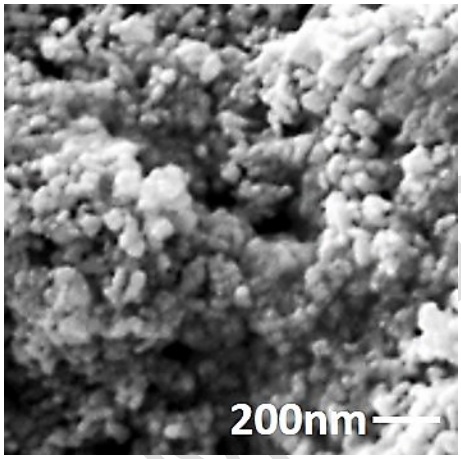


**Figure 2**. TEM image of biosynthesized Silver Nanoparticles

### 3.2 X-ray Diffractometer Analysis

The (111), (200), (220), (311), and (222) planes of crystallography of face-cantered cubic sterling silver nanoparticles were responsible for the identified spikes in the diffractogram at 39.25°, 45.32°, 65.89°, 76.17°, and 79.88°. Figure 3 shows that LI-AgNPs nanoparticles exhibit notable anisotropy because the reflected light at position (111) is significantly more intense than at different planes, which indicates that Ag0 absorption at this location throughout crystalline development was much improved. This dispersion structure was a good match for the typical JCPDS file no. 04-0783 scattering structure. These spikes for the nanosilver emulsion are currently documented in the scientific literature. A clear XRD spectrum dismissed the possibility of unreduced ions of silver or other contaminants being present without additional peaks [22]. According to the Debye-Scherrer formula, the mean particle dimension determined from the FWHM of the scattering spike was identified as 32 nm.

$$D = \frac{K\delta}{ßCos\Theta} \qquad (1)$$

D stands for crystal dimensions, δ is X-ray wavelength, and Θ is Bragg inclination. Figure 3 shows the XRD evaluation results.

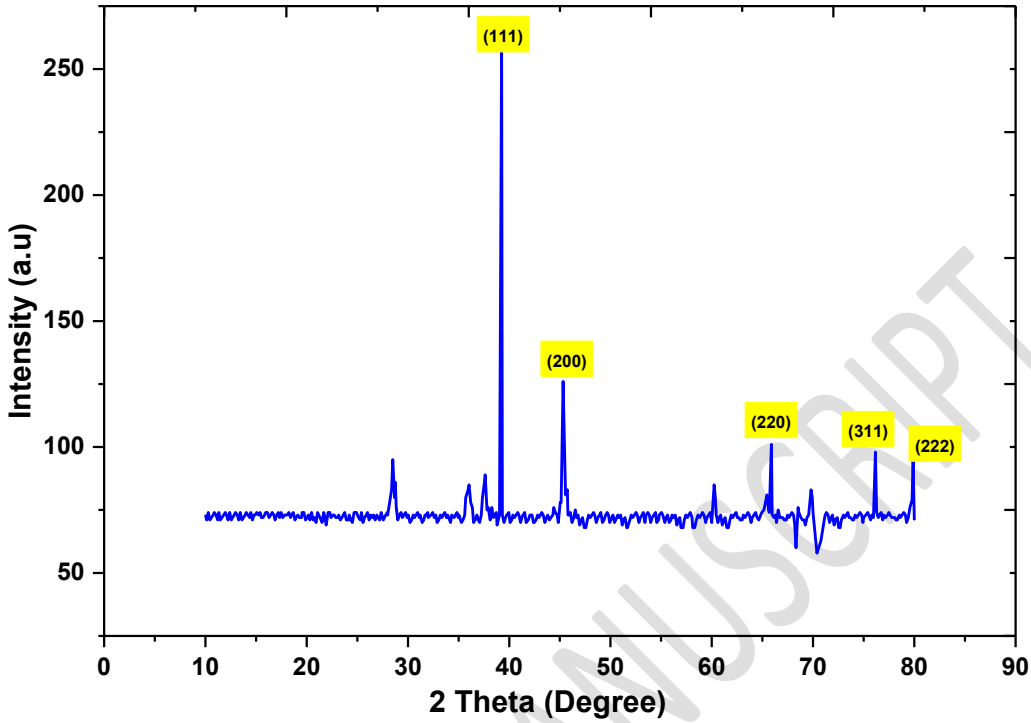


**Figure 3**. XRD Evaluation of biosynthesized Silver Nanoparticles from Lawsonia inermis leaf extract.



### 3.3 FTIR analysis

When making LI-AgNPs, LI extracts from leaves served as both an antioxidant and capsizing agent. Using the FTIR technique, shown in Figure 4. it was possible to determine the functional compounds and subsequent macromolecules associated with producing LI-AgNPs by eliminating Ag + ions. The molecules of water and protein components of the leaf extract were ascribed to a large spike at 3321 $cm^{-1}$ that corresponded to the overlapped stretching motion of the -$NH_2$ and -OH compounds. The detection of carbonyl straining in the proteins' amide connections could be attributed to the spectrum at 1718 $cm^{-1}$, while the linked doubly bonded vibratory stretching at 1580 $cm^{-1}$ suggested the existence of likely terpenoids or additional heterocyclic phytoconstituents [23].

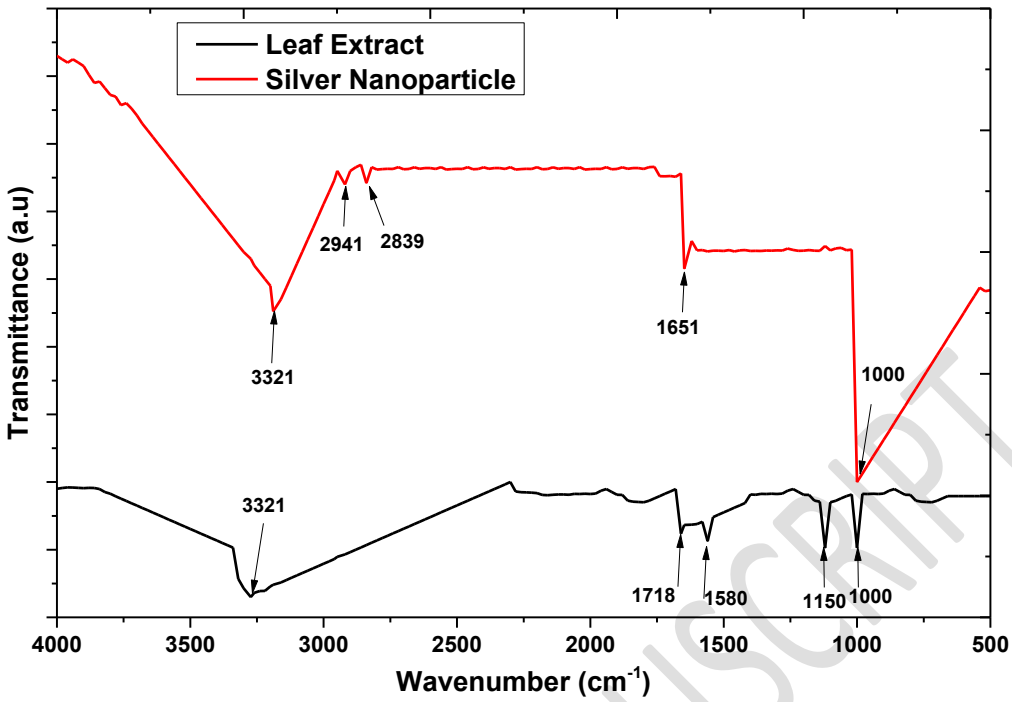


**Figure 3**. FTIR analysis of biosynthesized Silver Nanoparticles from Lawsonia inermis leaf extract

Bands between 1200 and 800 $cm^{-1}$ may be connected to the harmonics of the C-O molecule found in the components of flavonoids, proteins, or saccharides. The lipids, terpenoids, and enzymes found in LI leaf constituted the key contributors to these concentrations. When the spectra of LI-AgNPs and clean leaf extracts were compared, it became clear that a number of those categories played a role in creating and stabilizing nanoparticles because most of them either vanished or underwent significant positional alterations. In the LI-AgNPs spectra, two prominent bands reflected the -CH extension of saturation alkanes at 2941 and 2839 $cm^{-1}$. The process of reducing that underlies this effect is unknown, notwithstanding the well-established role of plant extracts as reducing agents in the biological creation of metallic nanoparticles [24]. According to research results, various plant metabolites are thought to contribute to bioreduction, subject to their origin. The hydroxyl, carbonyl, and amide groups that are found in the polyphenolic acidic substances, ketones, amino acids, and dietary components of LI leaf extract are thought to be mainly accountable for bio elimination in addition to restricting and stabilizing synthesized nanoparticles based on FTIR examination of LI-AgNPs.

### 3.4 Catalytic analysis of LI-AgNPs

In order to reduce four water-based biological pollutants—4-nitrophenol, eosin yellow, methyl blue, and methyl orange—the catalytic performance of synthesized silver nanoparticles,

LI-AgNPs, was examined. To ensure a precise assessment of the obtained data, every investigation was carried out at the substrate's pH value within atmospheric circumstances. The ability of as-produced LI-AgNPs to catalytically reduce 4NP by NaBH4 was assessed. The creation of a middle ion, the 4-nitrophenolate ion, which results in a red shift in the maximum concentration of 4NP in an alkaline solution, initiates the decline of 4NP (Figure 5). $H_3BO_3/BH_4$'s electrical potential is 1.34 V, whereas 4-NP/4-AP's E0 is 0.76 V compared to NHE. Although thermodynamically possible, the process is kinetically hampered by the substantial theoretical distinction between accepting and donating molecules. Silver nanoparticles effectively promoted electron transmission between the donor and acceptor molecules in these settings. The initial visible indication of the response's progression consisted of the yellow colour's fading with the progression of the response. A red-shifted absorption peak spanning 321 to 400 nm was used by spectroscopy to monitor the development of the reaction [25].

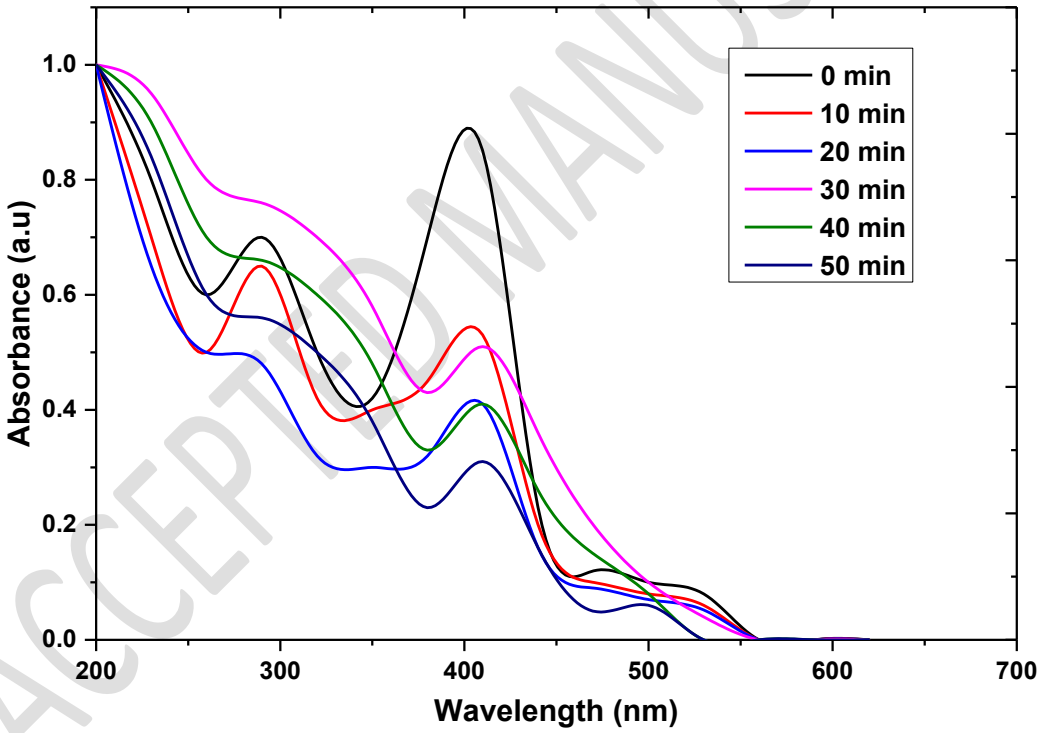


**Figure 5.** 0.45 mg/mL concentration of catalyst and UV-absorption spectrum of 4 nitrophenolate ion elimination in time

Figure 5 shows the sequential spectrum of absorption of the time-dependent diminution of the 4nitrophenolate ion initiated by LI-AgNPs at 400 nm. Peaks for 4NP and LI-AgNPs are depicted in the overlay figure. Using LI-AgNPs as a catalyst resulted in a sharp decrease in optical density and the emergence of an entirely novel concurrent spike at 320 nm, which was attributable to the consumption of the decreased item, 4-aminophenol. According to the

findings in Figure 6, LI-AgNPs served as an effective catalyst, reducing 4NP by 87% throughout the measured period, similar to the darkening of a yellow hue. By maintaining the same values for all of the additional variables, the amounts of LI-AgNPs were altered. Due to a larger variety of locations for reactions as concentrations rose, it was demonstrated that catalytic efficiency was dosage-dependent and improved [26]. Utilizing 0.45 mg/mL of catalyst, the greatest elimination of 4NP was accomplished. No additional rise in elimination was seen by improving the catalyst's level. According to speculation, the reaction most likely achieved equilibrium when more catalysts did not affect it (supplementary information). By contrasting the resultant absorbance peak (derived from the resulting solution) with a reference specimen containing 4AP, the decreased amount of 4NP was verified. Parallel experiments used freshwater rather than silver nanoparticles as a control medium [27, 28]. The catalyst function of LI-AgNPs was shown when it was discovered that the absorption region at 414 nm stayed practically intact and that less than 2.3% 4NP degradation continued after three days of exposure. It was shown that the existence of catalyst amounts of LI-AgNPs did not affect the absorption spectrum of 4NP. By reducing the decrease in potential, a significant quantity of the compound ion, a vigorous nucleophile, enhances the process of oxidizing silver particles. The co-adsorption of the compound and 4-nitrophenolate protons on the outermost portion of tiny silver particles is facilitated by the significant quantity of $NaBH_4$, which stimulates the nanosilver interface by reducing its oxide barrier backward.

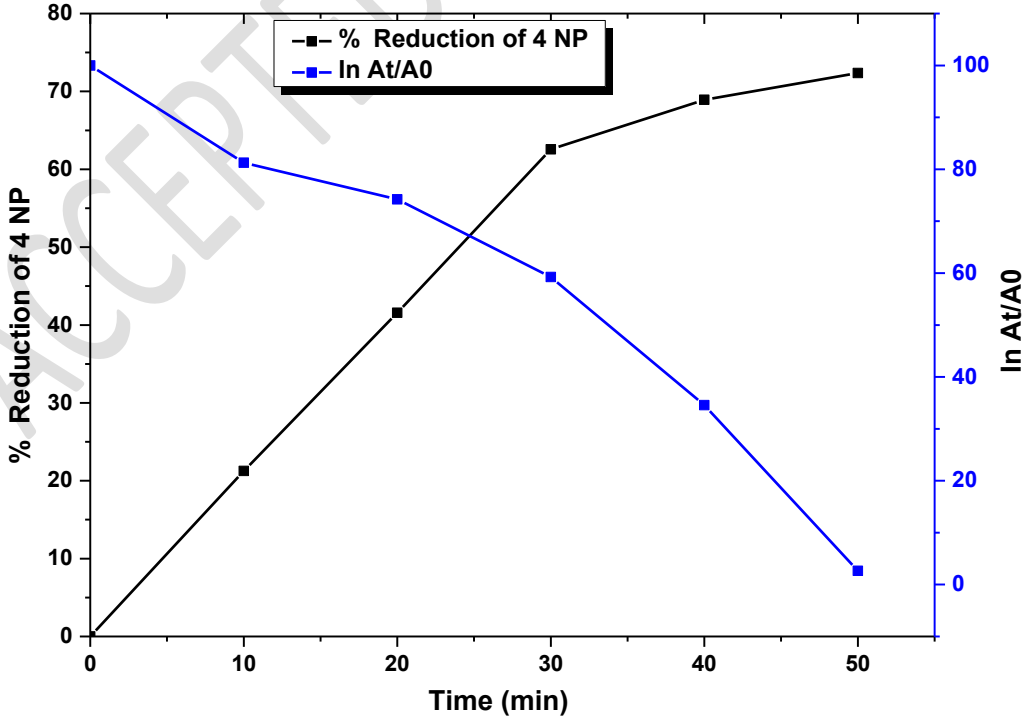

**Figure 6.** Rate of decrease and ln ($A_t/A_0$) plot of 4NP at a catalyst concentration of 0.45 mg/mL of LI-AgNPs

Furthermore, the resulting mixture's elevated pH prevents hydrogen ions from the borohydride ions from being released during the initial oxidizing of 4 aminophenol to return to 4NP. Although maintaining the other variables stable, an assortment of catalyst doses (0.15 mg/mL–0.45 mg/mL) had been used to test the catalytic capacity of LI-AgNPs for the decrease of methylene blue into leucomethylene blue by NaBH4 (supplementary material). Using an ultraviolet-visible spectrophotometer, an alteration in peak brightness at 611 nm was tracked to study the process of catalytic degradation. Findings revealed that dye elimination depended on the dose, and an increase in the percentage of catalyst was linked with a fast fall in the resultant mixture's absorbed effectiveness [29]. 50 minutes of contact at room temperature resulted in a 0.45 mg/mL catalytic load reduction of 72.36% of the MB. The response solution contained no LI-AgNPs in the preceding investigation, and the maximum intensity decreased by 2.89%. Three consecutive days of constant peak intensity in the control run demonstrated a relatively slow response rate. However, throughout 50 min, the reaction mixture including LI-AgNPs showed a considerable drop in the level of MB absorption, demonstrating that LI-AgNPs were chemically effective. Furthermore, hydrogen released from the compound ion protected the MB against airborne oxidation. By naturally mixing the reaction fluid and facilitating the dispersion of nanomaterials in the process, the small bubbles erupting from the outermost layer of the catalyst provided optimal circumstances for an effortless response. By naturally stirring the resultant solution and increasing the dispersion of nanomaterials in the reaction mixture, tiny air bubbles emerging from the outermost layer of the catalyst provided optimal circumstances for an even response.

As disodium saltwater, eosin yellow (ESH2) produces an orange solution in water-based media before becoming light yellow when reduced. Only 2.1% of the dyes decreased following three days when EY was decreased without LI-AgNPs due to a negligible drop in absorbance (data not shown). The strength of the peak for absorption rapidly decreased as the response progressed after the inclusion of LI-AgNPs. By observing the catalytic capacity for different catalytic levels, the impact of LI-AgNPs level on EY elimination was examined (supplementary information). At 0.45 mg/mL of catalytic level, which eliminated 73% of the initial colourant quantity, a saturation limit and maximal dye degradation were reached. The outcome highlighted how the catalytic function was influenced by concentration and enhanced with a higher catalytic dose. NaBH4 can decrease the azo dye methyl orange to create less harmful hydrazine derivatives. This work observed the typical MO absorbance spectrum at 466

nm to see how much it was reduced after 50 minutes of being subjected to different catalytic doses. A gradually declining MO absorbing point revealed the significant catalytic potential of LI-AgNPs. A concurrent new signal at 290 nm indicated the existence of hydrazine compounds also emerged. The catalytic loading with the greatest reported decrease kinetics, 0.2 mg/mL, removed 79.5% of the dye (supplementary results). Without a catalyst being present, there isn't a significant difference in peak strength during the entire time frame of the unaltered trial [30].

**3.5 Kinetic model of LI-AgNPs**

The subsequent pseudo-first-order rate formula was used to calculate the catalytic characteristics of the above reactions about the contaminant level.

$$kt = ln\left(\frac{A_t}{A_0}\right) \quad (2)$$

The rate at which it decreases may be considered independent of the level because $NaBH_4$ existed in the reaction product in considerably greater quantities than the contaminant. The value of absorbance at the beginning of the response, designated as A0, is identical to concentrations C0, and absorption at any point throughout intervals t, abbreviated as At, is comparable to concentrations Ct because the strength of the UV-visible absorption spike of the contaminants is directly correlated to their concentrations. Figure 6 demonstrates that for the decrease of 4NP, a strong linear correlation among ln (At/A0) and reduction duration in minutes was identified, indicating that the reactivity mechanisms maintained the pseudo-first-order kinetics [31, 32]. The sloping angles of the quadratic ln (At/A0) plots versus minute duration were utilized to compute the obvious constants for rates ($LI_{app}$). The spectrum of $LI_{app}$ values ranged between 0.0002-0.0361$min^{-1}$ (Table 1). The decrease of all contaminants at various levels was contrasted with the catalytic efficiency of LI-AgNPs. Pseudo's first-order kinetics could be seen in every plot. When used with MO, LI-AgNPs decreased dye by 81.42% at 0.2 mg/mL dosage in 50 minutes. For 4NP, the greatest rate stability was discovered at 0.45 mg/mL of LI-AgNPs, whereas for MB and EY, it was discovered at 0.45 mg/mL of loading. It has been demonstrated that the quantity of LI-AgNPs directly affects the catalyst reduction rate constants. When maintaining additional factors like the level of the contaminant and NaBH4 constant, it was discovered that the response rates were dosage proportional in every instance and rose continuously as one raised the amount of catalyst (Table 1). This may be explained by the fact that as the area needed for reactions grows, so does quantity [33].

**Table 1.** Contaminants Reduction based on the rate of LI AgNPs loading

| Contaminants | LI AgNPs (mg/ML) | LI $_{app}$ ($min^{-1}$) | Correlative Coefficients ($R^2$) |
|---|---|---|---|
| MO | 0 | 0.0065 | 0.921 |
| | 0.05 | 0.0043 | 0.983 |
| | 0.1 | 0.0062 | 0.971 |
| | 0.15 | 0.0132 | 0.956 |
| | 0.2 | 0.0213 | 0.984 |
| 4NP | 0 | 0.0002 | 0.965 |
| | 0.1 | 0.023 | 0.986 |
| | 0.2 | 0.029 | 0.984 |
| | 0.3 | 0.031 | 0.985 |
| | 0.4 | 0.0361 | 0.981 |
| | 0.45 | 0.0361 | 0.983 |
| EY | 0 | 0.0002 | 0.974 |
| | 0.1 | 0.012 | 0.976 |
| | 0.2 | 0.015 | 0.971 |
| | 0.3 | 0.016 | 0.897 |
| | 0.4 | 0.019 | 0.961 |
| | 0.45 | 0.019 | 0.972 |
| MB | 0 | 0.00072 | 0.961 |
| | 0.1 | 0.011 | 0.789 |
| | 0.2 | 0.013 | 0.785 |
| | 0.3 | 0.015 | 0.762 |
| | 0.4 | 0.018 | 0.861 |
| | 0.45 | 0.018 | 0.861 |



## 4. Conclusion

In summary, our investigation demonstrates the efficacy of aqueous Lawsonia inermis (LI) leaf extracts as a potent and cost-effective natural reduction agent for the eco-friendly synthesis of silver nanoparticles (LI-AgNPs). Characterization through UV-visible, HRTEM, SEM, XRD, and FTIR analyses confirms the predominantly spherical nature of the synthesized LI-AgNPs.

- Notably, in ambient conditions, the as-synthesized nanomaterials exhibit remarkable catalytic activity against specific non-biodegradable organic pollutants in water, including 4-nitrophenol (4NP), methylene blue (MB), eosin yellow (EY), and methyl orange (MO). The reduction processes are dosage-dependent, with the highest reduction efficiency observed for 4NP and the least for EY.
- Kinetic studies reveal that all reductive processes follow pseudo-first-order kinetics. Importantly, our findings establish a strong correlation between model predictions and experimental results, enabling the accurate prediction of pollution elimination at catalyst doses of 0.015 mg/mL.
- This study underscores the precise applications of LI leaf extract as a sustainable resource for the environmentally conscious synthesis of nanosilver colloids, showcasing its potential in efficiently reducing specific organic substances in wastewater treatment processes.

**5. Assessment of environmental impacts**

When treating wastewater with "Green Synthesis of Silver Nanoparticles using Lawsonia inermis for Enhanced Degradation of Organic Pollutants," it's important to consider how aquatic life may be impacted and how to reduce toxicity. The following are the precise impacts and strategies for removing potential toxicity:

**Effects on Aquatic Life:**

- Bioassays and Toxicity Testing: Conduct thorough biological tests and toxicity studies to determine how wastewater treatment affects aquatic creatures' well-being and behaviour.
- Monitoring Ecosystem Changes: Keep an eye out for any modifications to biodiversity, community organization, or general health of ecosystems when water that has been treated is released into aquatic environments.

**Mitigation of Toxicity:**

- Dilution and Dispersion: Before discharging wastewater that has been treated, lower the amount of silver nanoparticles (AgNPs) by implementing regulated diluting and dispersal procedures. By doing this, you may reduce your direct contact with aquatic life.
- Advanced filtering and Treatment: To eliminate or lessen the amount of AgNPs and other possible pollutants from the treated wastewater, use advanced filtering techniques or extra treatment procedures.

- Regulation and Monitoring: Create routine monitoring programmes to evaluate the wastewater treatment efficacy and guarantee that silver nanoparticle quantities are within regulatory bounds.

**Natural Attenuation Processes:**

- Sedimentation and Adsorption: Examine how AgNPs may become less available to aquatic species by sedimenting and adhering to particle materials in water bodies.
- Biological Degradation: Examine how naturally occurring microbial populations might break down or modify AgNPs, eventually reducing their toxicity.

Public Education and Awareness:

- Public Outreach Initiatives: Launch public education campaigns to inform the public about responsible utilization of nanomaterials and the significance of appropriate wastewater disposal procedures to reduce environmental harm.

These tactics can reduce harmful impacts on the aquatic environment and lessen the potential cytotoxicity of wastewater processed, including silver nanoparticles. Proper wastewater treatment must include periodic evaluation, respect for environmental rules, and a dedication to environmentally friendly procedures.

**6. Real time applications of Biosynthesized Nanoparticle**

Lawsonia inermis's green-synthesised silver nanoparticles, or AgNPs, have a lot of potential for practical uses in wastewater treatment. These nanoparticles' special qualities make them ideal for the following real-world situations:

- **Effective Wastewater Treatment:** The AgNPs have a strong catalytic effect on organic contaminants in water, including those that are not biodegradable. By adding these nanoparticles to wastewater treatment procedures, organic contaminants may be broken down more quickly, leading to a higher level of water purification.
- **Nano-Catalysis for Enhanced Degradation:** AgNPs' catalytic qualities may be used to support sophisticated oxidation procedures, which will effectively break down a variety of organic pollutants that are frequently present in wastewater, including phenols, dyes, and other contaminants.
- **Sustainable and Green Technology:** The synthesis of AgNPs using Lawsonia inermis complies with green and sustainable technology principles. This technique contributes to ecologically friendly wastewater treatment processes by providing an eco-friendly substitute for traditional nanoparticle manufacturing techniques.

- **Diminished Environmental effect:** The green synthesis process employing Lawsonia inermis will probably produce nanoparticles with less environmental effect than conventional chemical approaches. This is consistent with the increasing focus on creating technologies that reduce environmental footprints.
- **Versatile Use in a Variety of Water Treatment Facilities:** The adaptability of synthesised AgNPs allows them to be used in various water treatment facilities, from industrial effluent treatment systems to municipal wastewater treatment plants.
- **Integration with Current Treatment Technologies:** These nanoparticles may be included in current wastewater treatment systems, adding another level of effectiveness in removing persistent organic contaminants and improving the water quality.

In conclusion, Lawsonia inermis-derived green-synthesized silver nanoparticles provide a workable way to improve organic pollutant breakdown in actual wastewater treatment situations, providing water purification procedures with sustainability and efficacy.

**References**


[1]. Shankar VS, Velmurugan G, Raja DE, et al (2023) A Review on the Development of Silicon and Silica Based Nano Materials in the Food Industry. Silicon 1–10

[2]. Pandian et al., (2024). Analyzing the Moisture and Chemical Retention Behavior of Flax Fiber–Ceramic Hybrid Composites for Automotive Underbody Shields. SAE Technical Paper, (2024-01-5006), 1-8. https://doi.org/10.4271/2024-01-5006

[3]. Natrayan, L., & Kaliappan, S. (2023). Mechanical Assessment of Carbon–Luffa Hybrid Composites for Automotive Applications (No. 2023-01-5070). SAE Technical Paper.

[4]. Alhalili Z (2023) Metal Oxides Nanoparticles: General Structural Description, Chemical, Physical, and Biological Synthesis Methods, Role in Pesticides and Heavy Metal Removal through Wastewater Treatment. Molecules 28:3086

[5]. Saravanan A, Kumar PS, Hemavathy R V, et al (2022) A review on synthesis methods and recent applications of nanomaterial in wastewater treatment: Challenges and future perspectives. Chemosphere 135713

[6]. Aragaw TA, Bogale FM, Aragaw BA (2021) Iron-based nanoparticles in wastewater treatment: A review on synthesis methods, applications, and removal mechanisms. Journal of Saudi Chemical Society 25:101280

[7]. Raj TNV, Hoskeri PA, Hamzad S, et al (2022) Moringa Oleifera leaf extract mediated synthesis of reduced graphene oxide-vanadium pentoxide nanocomposite for enhanced

specific capacitance in supercapacitors. Inorganic Chemistry Communications 142:109648

[8]. El-Sayed AA, Amr A, Kamel OMHM, et al (2020) Eco-friendly fabric modification based on AgNPs@ Moringa for mosquito repellent applications. Cellulose 27:8429–8442

[9]. Sabarinathan et al., (2022) Experimental study on removal of phenol formaldehyde resin coating from the abrasive disc and preparation of abrasive disc for polishing application, Advances in Materials Science and Engineering, vol. 2022, 1-8. https://doi.org/10.1155/2022/6123160

[10]. Fouda A, Eid AM, Abdelkareem A, et al (2022) Phyco-synthesized zinc oxide nanoparticles using marine macroalgae, Ulva fasciata Delile, characterization, antibacterial activity, photocatalysis, and tanning wastewater treatment. Catalysts 12:756

[11]. Rambabu K, Bharath G, Banat F, Show PL (2021) Green synthesis of zinc oxide nanoparticles using Phoenix dactylifera waste as bioreductant for effective dye degradation and antibacterial performance in wastewater treatment. Journal of hazardous materials 402:123560

[12]. Hemanth et al., (2017). Evaluation of mechanical properties of E-Glass and coconut fiber reinforced with polyester and epoxy resin matrices. International journal of mechanical and production engineering research and development, 7(5), 13-20.

[13]. El-Sesy ME, Othman SA (2023) Promising antibacterial activities of anethole and green-synthesized magnetite nanoparticles against multiple antibiotic-resistant bacteria. Water Science and Technology 87:729–747

[14]. Devatha CP, Jagadeesh K, Patil M (2018) Effect of Green synthesized iron nanoparticles by Azardirachta Indica in different proportions on antibacterial activity. Environmental Nanotechnology, Monitoring & Management 9:85–94

[15]. Das C, Sen S, Singh T, et al (2020) Green synthesis, characterization and application of natural product coated magnetite nanoparticles for wastewater treatment. Nanomaterials 10:1615

[16]. Roy H, Islam MS, Arifin MT, Firoz SH (2022) Synthesis, Characterization and Sorption Properties of Biochar, Chitosan and ZnO-Based Binary Composites towards a Cationic Dye. Sustainability 14:14571

[17]. Rafique M, Shafiq F, Gillani SSA, et al (2020) Eco-friendly green and biosynthesis of copper oxide nanoparticles using Citrofortunella microcarpa leaves extract for efficient photocatalytic degradation of Rhodamin B dye form textile wastewater. Optik 208:164053

[18]. Ahmed T, Noman M, Shahid M, et al (2020) Green synthesis of silver nanoparticles transformed synthetic textile dye into less toxic intermediate molecules through LC-MS analysis and treated the actual wastewater. Environmental Research 191:110142

[19]. El-Aswar EI, Zahran MM, El-Kemary M (2019) Optical and electrochemical studies of silver nanoparticles biosynthesized by Haplophyllum tuberculatum extract and their antibacterial activity in wastewater treatment. Materials Research Express 6:105016

[20]. Lakshmaiya et al., (2023). Tanning Wastewater Sterilization in the Dark and Sunlight Using Psidium guajava Leaf-Derived Copper Oxide Nanoparticles and Their Characteristics. ACS Omega 2023, 8, 42, 39680–39689.

[21]. Ajitha B, Reddy YAK, Reddy PS, et al (2016) Instant biosynthesis of silver nanoparticles using Lawsonia inermis leaf extract: Innate catalytic, antimicrobial and antioxidant activities. Journal of Molecular Liquids 219:474–481. https://doi.org/10.1016/j.molliq.2016.03.041

[22]. Agarwal P, Gupta R, Agarwal N (2019) Advances in synthesis and applications of microalgal nanoparticles for wastewater treatment. Journal of Nanotechnology 2019:

[23]. Anand S, Lamba J, Sharma PK, et al (2023) Azolla microphylla extract ZnO nanoparticles and antibacterial activity: eco-friendly wastewater treatment. Nanotechnology for Environmental Engineering 8:183–195

[24]. Hamad MT (2019) Biosynthesis of silver nanoparticles by fungi and their antibacterial activity. International Journal of Environmental Science and Technology 16:1015–1024

[25]. Babavali et al., (2023). Thermal management of PV panel through the circulation of a nano-MgO/water-based nanofluid. Materials Today: Proceedings. Vol. 93, pp 1-6. DOI: 10.1016/j.matpr.2023.09.001

[26]. Velmurugan, G., & Natrayan, L. (2023). Experimental investigations of moisture diffusion and mechanical properties of interply rearrangement of glass/Kevlar-based hybrid composites under cryogenic environment. Journal of Materials Research and Technology, 23, 4513-4526. https://doi.org/10.1016/J.JMRT.2023.02.089

[27]. Vasantharaj S, Sathiyavimal S, Senthilkumar P, et al (2021) Enhanced photocatalytic degradation of water pollutants using bio-green synthesis of zinc oxide nanoparticles (ZnO NPs). Journal of Environmental Chemical Engineering 9:105772

[28]. Preetha BK, Vishalakshi B (2020) Microwave assisted synthesis of karaya gum based montmorillonite nanocomposite: Characterisation, swelling and dye adsorption studies. International Journal of Biological Macromolecules 154:739–750

[29]. Abegunde SM, Idowu KS, Sulaimon AO (2020) Plant-mediated iron nanoparticles and their applications as adsorbents for water treatment–a review. J Chem Rev 2:103–113

[30]. Wei S, Wang Y, Tang Z, et al (2020) A size-controlled green synthesis of silver nanoparticles by using the berry extract of Sea Buckthorn and their biological activities. New Journal of Chemistry 44:9304–9312

[31]. Ismail GA, Allam NG, El-Gemizy WM, Salem MA (2021) The role of silver nanoparticles biosynthesized by Anabaena variabilis and Spirulina platensis cyanobacteria for malachite green removal from wastewater. Environmental Technology 42:4475–4489

[32]. Choudhary MK, Kataria J, Sharma S (2018) Evaluation of the kinetic and catalytic properties of biogenically synthesized silver nanoparticles. Journal of cleaner production 198:882–890

[33]. Karthiga Devi G, Senthil Kumar P, Sathish Kumar K (2016) Green synthesis of novel silver nanocomposite hydrogel based on sodium alginate as an efficient biosorbent for the dye wastewater treatment: prediction of isotherm and kinetic parameters. Desalination and Water Treatment 57:27686–27699